Photochemical & Photobiological Sciences

PAPER

View Article Online
View Journal

Cite this: DOI: 10.1039/c8pp00109j

Photobiomodulation prevents DNA fragmentation of alveolar epithelial cells and alters the mRNA levels of caspase 3 and Bcl-2 genes in acute lung injury

Luiz Philippe da Silva Sergio, *[a] Andrezza Maria Côrtes Thomé,[a] Larissa Alexsandra da Silva Neto Trajano,[b] Andre Luiz Mencalha,[a] Adenilson de Souza da Fonseca[a,d,e] and Flávia de Paoli[c]

Acute respiratory distress syndrome (ARDS) and acute lung injury (ALI) are defined as pulmonary inflammation that could occur from sepsis and lead to pulmonary permeability and alveolar edema making them life-threatening diseases. Photobiomodulation (PBM) properties have been widely described in the literature in several inflammatory diseases; although the mechanisms of action are not always clear, this could be a possible treatment for ARDS/ALI. Thus, the aim of this study was to evaluate the mRNA levels from caspase-3 and BCL-2 genes and DNA fragmentation in lung tissue from *Wistar* rats affected by ALI and subjected to photobiomodulation by exposure to a low power infrared laser (808 nm; 100 mW; 3.571 W cm^{-2}; four points per lung). Adult male *Wistar* rats were randomized into 6 groups (n = 5, for each group): control, PBM10 (10 J cm^{-2}, 2 J and 2 seconds), PBM20 (20 J cm^{-2}, 5 J and 5 seconds), ALI, ALI + PBM10 and ALI + PBM20. ALI was induced by intraperitoneal *Escherichia coli* lipopolysaccharide injection. Lung samples were collected and divided for mRNA expression of caspase-3 and Bcl-2 and DNA fragmentation quantifications. Data show that caspase-3 mRNA levels are reduced and Bcl-2 mRNA levels increased in ALI after low power infrared laser exposure when compared to the non-exposed ALI group. DNA fragmentation increased in inflammatory infiltrate cells and reduced in alveolar cells. Our research shows that photobiomodulation can alter relative mRNA levels in genes involved in the apoptotic process and DNA fragmentation in inflammatory and alveolar cells after lipopolysaccharide-induced acute lung injury. Also, inflammatory cell apoptosis is part of the photobiomodulation effects induced by exposure to a low power infrared laser.

Received 14th March 2018,
Accepted 4th June 2018

DOI: 10.1039/c8pp00109j

rsc.li/pps

Introduction

Acute respiratory distress syndrome is characterized by acute pulmonary inflammation, most frequently caused by infections.[1] In this condition, pulmonary permeability increases, causing alveolar edema, which in turn impairs gas exchange.[1] From the 2012 Berlin definition, acute respiratory distress syndrome and acute lung injury (ALI) became the spectra of the same disease in which the severity of the syndrome was stratified according to the PaO_2/FiO_2 ratio in three categories: mild (200–300 mmHg), moderate (100–200 mmHg) and severe (<100 mmHg with a minimum level of 5 cm H_2O of PEEP – positive end-expiratory pressure).[2] An early diagnosis is important to implement other strategies in addition to supporting the respiratory function as well as other organs affected by sepsis, in order to minimize potential damage[3] and to reduce mortality, which remains high, surpassing 40% in the severe category.[2]

[a]*Departamento de Biofísica e Biometria, Instituto de Biologia Roberto Alcantara Gomes, Universidade do Estado do Rio de Janeiro, Avenida 28 de Setembro, 87, fundos, Vila Isabel, Rio de Janeiro, 20551030, Brazil.*
E-mail: luizphilippesergio@gmail.com; Fax: +55 21 23342058; Tel: +55 21 23342058
[b]*Laboratório de Biomorfologia e Patologia Experimental, Mestrado Profissional em Ciências Aplicadas em Saúde, Universidade Severino Sombra. Avenida Expedicionário Oswaldo de Almeida Ramos, 280, Vassouras, Rio de Janeiro, 27700000, Brazil*
[c]*Departamento de Morfologia, Instituto de Ciências Biológicas, Universidade Federal de Juiz de Fora, Rua José Lourenço Khelmer – s/n, Campus Universitário, São Pedro, Juiz de Fora, Minas Gerais, 36036900, Brazil*
[d]*Departamento de Ciências Fisiológicas, Instituto Biomédico, Universidade Federal do Estado do Rio de Janeiro, Rua Frei Caneca, 94, Rio de Janeiro, 20211040, Brazil*
[e]*Centro de Ciências da Saúde, Centro Universitário Serra dos Órgãos, Avenida Alberto Torres, 111, Teresópolis, Rio de Janeiro, 25964004, Brazil*

Inflammatory response plays a critical role in acute respiratory distress syndrome pathophysiology, from the activation of alveolar macrophages which results in the secretion of cytokines and neutrophils and in circulating macrophage recruitment into lungs.[4] Inflammation onset leads to endothelium and epithelium rupture, establishing alveolar edema and compromising gas exchange.[5]

In general, polymorphonuclear cells are very short half-life cells; however, in inflammatory processes, death by apoptosis is prevented by inflammatory signal.[6] Subsequently, this mediates apoptotic polymorphonuclear cell clearance by macrophages,[6] putting an end to the inflammation and restoring tissue homeostasis.[7] Two major signaling pathways are involved in polymorphonuclear cell apoptosis: the death receptor or the extrinsic pathway (Fas and Fas binding-FasL), and the mitochondrial or intrinsic pathway (pro-apoptotic Bcl-2 family of the protein, such as Bax).[8] Both pathways result in the release of cytochrome c and the mitochondrial outer membrane permeabilization, which trigger events of apoptosis by caspases. DNA fragmentation by endonucleases and cytoskeleton reorganization are promoted by effector caspases (caspase 3, for example), resulting in apoptotic body formation.[9,10] However, cellular resistance to apoptotic stimuli is due to the balance between anti-apoptotic proteins (Bcl-2, Bcl-x, Bcl-XL, Bcl-XS, Bcl-w and BAG) and pro-apoptotic proteins (Bax, Bak, Bid, Bad, Bim, Bik, and Blk).[11]

A previous study showed apoptosis participation in the photobiomodulation effects on the inflammatory process.[12] The photobiomodulation effect induced by low power lasers is related to the monochromatic and collimated characteristics of laser beams,[13] which allow photon absorption by a specific photoacceptor[14] This effect has been reported to accelerate tissue repair and analgesia.[15,16] Also, photobiomodulation has been described in cells associated with inflammatory response and tissue repair, such as lymphocytes,[17] fibroblasts,[18] macrophages,[19] in the movement of red blood cells,[20] as well as in blood plasma components, such as hemoglobin, immunoglobulins and proteins,[21] cell growth factors[22] and cytokines.[23]

Although therapeutic protocols have been used successfully, the mechanism of action of photobiomodulation has not been understood. Photobiomodulation effects by low power lasers have been observed in several types of cells, tissues and organs. However, the photobiomodulation effects on inflammatory pulmonary diseases are poorly explored as well as the evaluation of the apoptosis profile in inflammatory cells and pulmonary parenchyma in animals affected by acute lung injury and subjected to photobiomodulation. Additionally, the mRNA evaluation from genes related to apoptosis and DNA fragmentation can provide information about the inflammatory process resolution and the state of the lung parenchyma in experimental models of acute lung injury. Thus, the objective of this study was to evaluate the photobiomodulation effects on the relative levels of caspase-3 and Bcl-2 mRNA, as well as cellular fragmentation of alveolar and inflammatory cells from *Wistar* rats affected by acute lung injury. The laser fluences, power and emission mode were those used in clinical protocols for inflammatory disease treatment.

Experimental

Animals

Experiments were conducted in accordance with the Ethics Committee in Animal Experiments of Universidade Federal de Juiz de Fora, Minas Gerais, Brazil, protocol number 012/2016. Twenty four adult male *Wistar* rats (weighing 285.0 ± 22.9 g) were obtained from the Departamento de Ciências Fisiológicas vivarium (Universidade Federal do Estado do Rio de Janeiro – Brazil). Over the week before the experiment, groups of five animals were housed in clear plastic cages with stainless steel wire lids and pinewood shavings as bedding. Additionally, the animals were kept in an animal room with controlled environmental conditions (12 h light/12 h dark cycle, temperature 22 °C) on closed ventilated shelves. Animals received rat chow pellets and water *at libitum*.

Low power laser

A therapeutic low power infrared laser (Photon Lase III) purchased from D.M.C. Equipamentos Ltda (São Paulo, Brazil) was used in this study. The laser parameters are presented on Table 1.

Reagents

Escherichia coli lipopolysaccharide (LPS) serotype 055:B5 was from Sigma-Aldrich (USA), TRIzol® reagent was secured from Invitrogen (USA); isopropanol, chloroform and ethanol from Merck (Germany); diethyl pyrocarbonate (DEPC) from Sigma (USA); NaCl (sodium chloride) purchased from Vetec (Rio de Janeiro, Brazil) and Entellan (Roche, Germany).

Experimental procedure

Animals were anesthetized with intraperitoneal bolus of ketamine (80 mg kg^{-1}) and xylazine (8 mg kg^{-1})[24] and then, randomly assigned to six main groups of five animals each: (1) C (Control) were animals treated with intraperitoneal saline solution (0.9% NaCl); (2) PBM10 were animals treated with intraperitoneal saline solution and exposed to an infrared laser at 10 J cm^{-2}; (3) PBM20 were animals treated with intraperitoneal saline solution and exposed to an infrared laser at 20 J cm^{-2};

Table 1 Photobiomodulation physical parameters

Wavelength (nm)	808
Diode laser	AsGaAl
Power (mW)	100
Spot size (cm^2)	0.028
Power density (W cm^{-2})	3.571
Energy per point (J)	2 and 5
Energy density (J cm^{-2})	10 and 20
Time per point (s)	2 and 5
Number of points per lung	4
Application technique	Punctual by skin contact
Number of treatment sessions	One session

(4) ALI (acute lung injury) were animals treated with intraperitoneal LPS (10 mg kg^{-1}); (5) ALI-PBM10 were animals treated with intraperitoneal LPS (10 mg kg^{-1}) and, after 4 hours, exposed to an infrared laser at 10 J cm^{-2}; (6) ALI-PBM20 were animals treated with intraperitoneal LPS (10 mg kg^{-1}) and, after 4 hours, exposed to an infrared laser at 20 J cm^{-2}. LPS solutions were prepared in saline solution immediately before use to induce ALI.

Irradiation procedure occurred after sedation with intraperitoneal bolus of ketamine (80 mg kg^{-1}) and xylazine (8 mg kg^{-1}), dorsal decubitus position and tricotomy of the thoracic region of the *Wistar* rats, determined four points between the ribs along each lung. Low power infrared laser exposure occurred after 4 hours of ALI induction. After 24 hours of LPS-induced ALI or after exposure to an infrared laser, animals were euthanized with anesthetic overdose and laparotomy was performed. The trachea was clamped and lungs removed for further analysis.

Evaluation of relative mRNA levels of DNA repair genes

Procedure. After euthanasia, samples (50 up to 100 mg) from right lung tissue were collected and transferred to microcentrifuge flex tubes with TRIzol® reagent for total RNA extraction by a standard procedure.

Total RNA extraction and complementary DNA synthesis. Tissue samples were crushed into microcentrifuge flex tubes with TRIzol® reagent and centrifuged (12 000*g*, 4 °C, 10 minutes). Supernatants were transferred to other tubes, chloroform added, mixtures centrifuged (12 000*g*, 4 °C, 15 minutes), aqueous phases transferred to other tubes and isopropanol added. After incubation (room temperature, 15 minutes), mixtures were centrifuged (12 000*g*, 4 °C, 10 minutes), supernatants discarded and the precipitate washed with ethanol–DEPC (80% ethanol, DEPC 0.1%) solution and centrifuged. Supernatants were withdrawn and total RNA reconstituted in water–DEPC (0.1%) solution and stored (−80 °C).

RNA concentration and purity were determined with a spectrophotometer by calculating the optical density ratio at a 260/280 nm wavelength ratio. Complementary DNA (cDNA) synthesis was carried out using a two-step cDNA synthesis kit (Promega, USA). Four micrograms of RNA were reverse transcribed into cDNA using GoScript™ reverse transcriptase (Promega, USA), according to the manufacturer's protocol, using a total 20 μL reaction. Real-time quantitative polymerase chain reaction (RT-qPCR) was performed using 5 μL of GoTaq qPCR Master Mix (Promega, USA) for a final volume of 10 μL volume containing 50 ng of cDNA. Samples were amplified with caspase 3, B-cell lymphoma 2 (Bcl-2) and glyceraldehyde-3-phosphate dehydrogenase (GAPDH) primers to determine the initial relative cDNA quantity. Reactions, in duplicate for each sample, were run on an Applied Biosystems 7500 RT-qPCR machine (Applied Biosystems, USA). The PCR was initially denatured at 94 °C for 10 minutes, followed by 40 cycles of denaturation at 94 °C for 30 s, annealing at 60 °C for 30 s (except for OGG1, whose annealing step was 67 °C for 30 s) and an extension period at 72 °C for 30 s. Melt curve analyses were performed for all genes and PCR product specificity was confirmed by the presence of a single peak. Relative expression was normalized by reference gene levels (GAPDH) using ALI rats from the control group. Duplicate Ct values were analyzed in Microsoft Excel (Microsoft) using the comparative Ct ($2^{-\Delta\Delta CT}$) method.[25]

DNA fragmentation. After euthanasia, samples from left lung tissues were collected and fixed (4% buffered formaldehyde, 0.01 M, pH 7.4) and processed for paraffin embedding. Four-micrometer thick sagittal slices were taken. DNA fragmentation in *Wistar* rats lung samples was detected using a TUNEL (terminal deoxynucleotidyl transferase-mediated 2′-deoxyuridine, 5′-triphosphate nick-end-labeling) assay (Roche, Germany) according to the manufacturer's manual. After deparaffinization and permeabilization, tissue sections were incubated in proteinase K for 15 minutes at room temperature. The sections were then incubated with a TUNEL reaction mixture which contains terminal deoxynucleotidyl transferase and fluorescein-dUTP at 37 °C for 1 hour. After washing three times with PBS, the sections were incubated with the Converter-POD containing anti-fluorescein antibody conjugated with horse-radish peroxidase (POD) at room temperature for 30 minutes. After washing three times with PBS, the sections were incubated with 3-3′-diaminobenzidine (Sigma Aldrich, USA) for 10 minutes at room temperature (25 °C), and then counterstained using Herry's haematoxylin. The preparations were air dried and mounted in Entellan. Quantitative analyses were performed using a conventional light micro Carl Zeiss Axio Lab. A1 microscope, equipped with an Axiocam ERc5S Rev. 2.0–20/0.40 objective, captured with a 5 M color video, using Zen 2 (blue edition) software (Zeiss, Germany).

Statistical analysis

Data normality was ascertained by Kolmogorov–Smirnov test. Parametric data were expressed as mean ± standard deviation and non-parametric data were expressed as median (interquartile range). Mann Whitney test was performed to compare the data from the ALI group with the control group. This comparison was performed using data normalization with the control group. One-way ANOVA followed by Bonferroni's multiple comparison tests were used to compare parametric data and for nonparametric data, Kruskal–Wallis followed by Dunn's multiple comparison test. Relative mRNA level data were normalized with the control group to compare the animals exposed to a low power infrared laser with the animals from the control group. Relative mRNA level data were normalized with the the ALI group to compare the animals affected by ALI with the animals affected by ALI and exposed to a low power infrared laser. $p < 0.05$ was considered as the less significant level. InStat Graphpad software was used to perform statistical analysis (GraphPad InStat version 5.0 for Windows 8, GraphPad Prism Software, San Diego, CA, USA).

Results

Relative caspase 3 and Bcl-2 mRNA levels in lung tissue from normal and LPS-induced ALI

Data in Fig. 1A show a significant ($p < 0.001$) increase of relative caspase 3 mRNA levels in lung tissue from the animals from the ALI group when normalized and compared with the control group. Fig. 1B shows a significant ($p < 0.001$) decrease of Bcl-2 in lung tissue from rats after LPS-induced ALI when normalized and compared with the control group.

Relative caspase 3 and Bcl-2 mRNA levels in lung tissue from LPS-induced ALI animals subjected to photobiomodulation

Fig. 2 shows the relative caspase 3 mRNA levels in lung tissue after LPS-induced ALI and photobiomodulation by exposure to a low power infrared laser at different fluences (10 and 20 J cm^{-2}). Data in this figure indicate no significant ($p > 0.05$) alteration of relative caspase 3 mRNA levels in lung tissue from normal rats exposed to a low power infrared laser at both fluences evaluated (10 and 20 J cm^{-2}) when normalized and compared with the control group (Fig. 2A). However, a significant decrease ($p < 0.001$) of relative caspase 3 mRNA levels was obtained in lung tissue from rats after LPS-induced ALI and photobiomodulation at both fluences when normalized and compared with the LPS-induced ALI group (Fig. 2B).

Fig. 3 shows the relative Bcl-2 mRNA levels in lung tissue after LPS-induced ALI and photobiomodulation (10 and 20 J cm^{-2}). Similar to Fig. 2, data in this figure indicate no significant ($p > 0.05$) alteration of relative Bcl-2 mRNA levels in lung tissue from normal rats subjected to photobiomodulation (10 and 20 J cm^{-2}) when normalized and compared with the control group (Fig. 3A). However, a significant increase of relative Bcl-2 mRNA levels was obtained in lung tissue from rats after LPS-induced ALI and photobiomodulation at fluences 10 and 20 J cm^{-2} ($p < 0.05$ and $p < 0.01$, respectively) when normalized and compared with the LPS-induced ALI group (Fig. 3B).

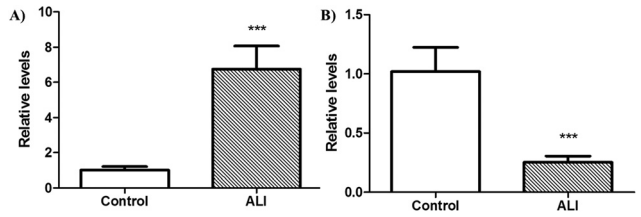

Fig. 1 (A) and (B) Relative mRNA levels from caspase 3 and Bcl-2 respectively from normal and acute lung injury. *Wistar* rats were inoculated with lipopolysaccharide and after 4 hours, they were exposed to a low power infrared laser at different fluences. Right lungs were collected, total RNA extraction, complementary DNA synthesis and real-time quantitative polymerase chain reaction were performed. The assay was carried out according to the manufacturer's manual. ***$p < 0.001$ when compared to the control group.

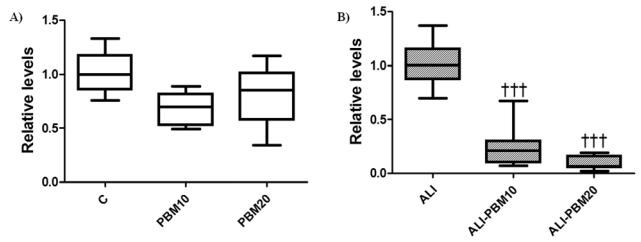

Fig. 2 Relative caspase 3 mRNA level in lung tissue after acute lung injury by lipopolysaccharide and photobiomodulation. *Wistar* rats were inoculated with lipopolysaccharide and after 4 hours, they were exposed to a low power infrared laser at different fluences. Right lungs were collected, total RNA extraction, complementary DNA synthesis and real-time quantitative polymerase chain reaction were performed according to the manufacturer's manual. Groups: C (control), PBM10 (photobiomodulation at 10 J cm^{-2}), PBM20 (photobiomodulation at 20 J cm^{-2}); acute lung injury (ALI), ALI-PBM10 (acute lung injury and photobiomodulation at 10 J cm^{-2}), ALI-PBM20 (acute lung injury and photobiomodulation at 20 J cm^{-2}). GAPDH was used as an internal standard for normalization and the ALI group was used as the second normalizer (ΔΔCt). $^{†††}p < 0.001$ when compared to the ALI group. ALI: acute lung injury. PBM: photobiomodulation. GAPDH: glyceraldehyde-3-phosphate dehydrogenase.

DNA fragmentation rate in alveolar and inflammatory cells in lung tissue from normal and LPS-induced ALI

Representative images from positive labeling for DNA fragmentation in lung cells are demonstrated in Fig. 4. This labeling was predominantly on inflammatory cells in the ALI group. Furthermore, these images demonstrated that LPS-induced ALI was successful.

DNA fragmentation rate in alveolar and inflammatory cells in lung tissue

In order to ascertain the type of cells involved in the DNA fragmentation and apoptosis process, the pulmonary architecture

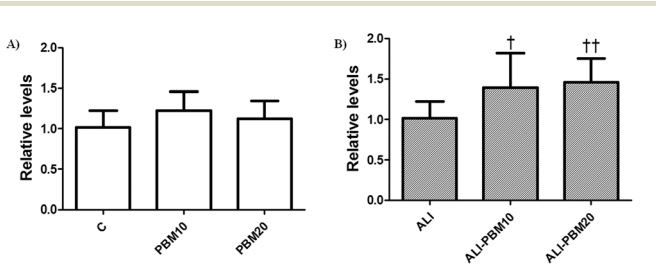

Fig. 3 Relative Bcl-2 mRNA level in lung tissue after acute lung injury by lipopolysaccharide and photobiomodulation. *Wistar* rats were inoculated with lipopolysaccharide and after 4 hours, exposed to a low power infrared laser at different fluences. Right lungs were collected, total RNA extraction, complementary DNA synthesis and real-time quantitative polymerase chain reaction performed according to the manufacturer's manual. Groups: C (control), PBM10 (photobiomodulation at 10 J cm^{-2}), PBM20 (photobiomodulation at 20 J cm^{-2}); acute lung injury (ALI), ALI-PBM10 (acute lung injury and photobiomodulation at 10 J cm^{-2}), ALI-PBM20 (acute lung injury and photobiomodulation at 20 J cm^{-2}). GAPDH was used as an internal standard for normalization, and the ALI group used as the second normalizer (ΔΔCt). $^{†}p < 0.05$ and $^{††}p < 0.01$ when compared to the ALI group. ALI: acute lung injury. PBM: photobiomodulation. GAPDH: glyceraldehyde-3-phosphate dehydrogenase.

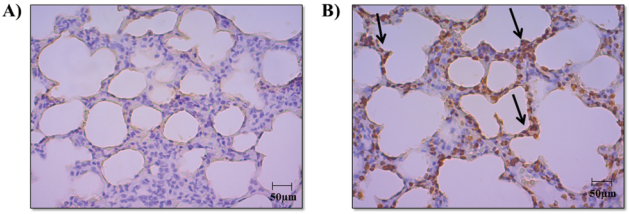

Fig. 4 Representative images from normal (left) and acute lung injury (right) lungs. *Wistar* rats were inoculated with lipopolysaccharide and after 4 hours, they were exposed to a low power infrared laser at different fluences. Left lungs were collected, fixed, processed for paraffin and the terminal deoxynucleotidyl transferase-mediated 2′-deoxyuridine, 5′-triphosphate nick-end-labeling assay performed. The assay was carried out according to the manufacturer's manual. Arrow indicates positive labeling to DNA fragmentation, especially in PMN cells.

was evaluated 24 hours after LPS-induced ALI and photobiomodulation.

Fig. 5 shows no alteration ($p > 0.05$) of positive labeling in pulmonary tissue from normal rats subjected to photobiomodulation by exposure to a low power infrared laser at different fluences (10 and 20 J cm^{-2}) when compared to the control group. However, following LPS-induced ALI, an increase ($p < 0.001$) of positive labeling on alveolar cells was observed. On the other hand, after photobiomodulation, there was a significant decrease ($p < 0.001$) of positive labeling on alveolar cells in lung tissue at both the low power infrared laser fluences evaluated.

Fig. 6 shows no alteration ($p > 0.05$) of positive labeling from normal rats subjected to photobiomodulation (10 and 20 J cm^{-2}) when compared to the control group. On the other hand, LPS-induced ALI was observed to significantly ($p < 0.001$) increase the positive labeling on inflammatory cells.

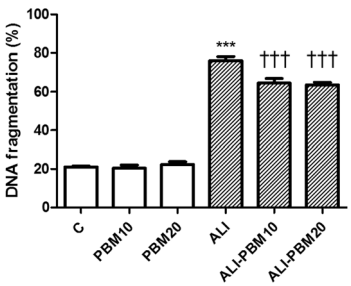

Fig. 5 Percentage of DNA fragmentation in alveolar cells. *Wistar* rats were inoculated with lipopolysaccharide and after 4 hours, they were exposed to a low power infrared laser at different fluences. Left lungs were collected, fixed, processed for paraffin and terminal deoxynucleotidyl transferase-mediated 2′-deoxyuridine, 5′-triphosphate nick-end-labeling assay performed according to the manufacturer's manual. Groups: C (control), PBM10 (photobiomodulation at 10 J cm^{-2}), PBM20 (photobiomodulation at 20 J cm^{-2}); acute lung injury (ALI), ALI-PBM10 (acute lung injury and photobiomodulation at 10 J cm^{-2}), ALI-PBM20 (acute lung injury and photobiomodulation at 20 J cm^{-2}). ***$p < 0.001$ when compared to the control group and $^{\dagger\dagger\dagger}p < 0.001$ when compared to the ALI group. ALI: acute lung injury. PBM: photobiomodulation.

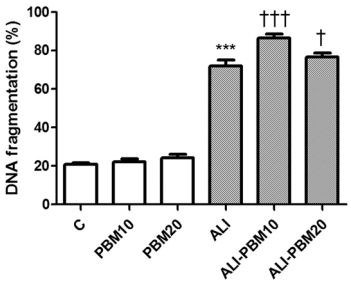

Fig. 6 Percentage of DNA fragmentation in the infiltrated area. *Wistar* rats were inoculated with lipopolysaccharide and after 4 hours, they were exposed to a low power infrared laser at different fluences. Left lungs were collected, fixed, processed for paraffin and the terminal deoxynucleotidyl transferase-mediated 2′-deoxyuridine, 5′-triphosphate nick-end-labeling assay was performed according to the manufacturer's manual. Groups: C (control), PBM10 (photobiomodulation at 10 J cm^{-2}), PBM20 (photobiomodulation at 20 J cm^{-2}); acute lung injury (ALI), ALI-PBM10 (acute lung injury and photobiomodulation at 10 J cm^{-2}), ALI-PBM20 (acute lung injury and photobiomodulation at 20 J cm^{-2}). ***$p < 0.001$ when compared to the control group and $^{\dagger}p < 0.05$ and $^{\dagger\dagger\dagger}p < 0.001$ when compared to the ALI group. ALI: acute lung injury. PBM: photobiomodulation.

Also, there was a significant increase of positive labeling on inflammatory cells in lung tissue from rats following LPS-induced ALI and photobiomodulation by exposure to a low power infrared laser at fluences of 10 and 20 J cm^{-2} ($p < 0.001$ and $p < 0.05$, respectively) when compared to those in the lungs from rats after LPS-induced ALI but not those subjected to photobiomodulation.

Discussion

Photobiomodulation is used for the treatment of a number of diseases, such as inflammatory diseases,[26,27] because the photobiomodulation effect is considered a safe and effective approach.[28] Some authors have demonstrated the anti-inflammatory effect of photobiomodulation by exposure to a low power red laser (660 nm),[29] low power infrared laser,[30] white LED (light emitting diode)[31] and red and infrared LED (630 and 870 nm)[32] under modulation inflammatory mediators.[33] However, a low power infrared laser (808 nm) was used due to the generation of a longer and narrow volume of coherent radiation,[34,35] whose penetration capacity is able to reach deeper tissues,[36] reaching lung tissue.

A number of studies have reported an anti-inflammatory effect by regulation of pro-inflammatory mRNAs induced by photobiomodulation by exposure to low power lasers, but this effect depends on laser parameters, such as fluence.[37] Also, photobiomodulation could induce or inhibit apoptosis.[12] Neutrophils and epithelial cells are two of the major cells that undergo apoptosis in acute respiratory distress syndrome. Intra-alveolar neutrophil apoptosis has been reported[38,39] as well as structural alterations due to pneumocyte apoptosis.[40,41]

Induction of acute lung injury (ALI) or acute respiratory distress syndrome by lipopolysaccharide (LPS) has been a successful experimental model for ALI, being used in several studies.[42–44] Thus, this experimental model was used for the evaluation of the photobiomodulation effect on apoptosis in acute lung injury.

Relative mRNA levels from genes related to apoptosis have been evaluated by real-time reverse transcription polymerase chain reaction (RT-qPCR) in cell cultures, as well as biological tissues.[12,45] These studies have allowed understanding the factors and conditions that could modify the expression of these genes. This technique is considered the gold standard for measuring mRNA expression relative to a reference mRNA (from GAPDH gene, for example).[46] In addition, the terminal deoxynucleotidyl transferase-mediated 2′-deoxyuridine,5′-triphosphate nick-end-labeling (TUNEL) assay is the gold standard used to reveal DNA fragmentation by the presence of a large number of DNA strand breaks, hence usually used for the identification of apoptotic cells.[47,48]

Caspase 3 and Bcl-2 act on the induction and protection of apoptotic cells, respectively.[11] Our results show an increase in relative caspase 3 mRNA levels and a DNA fragmentation increase in lung tissue from *Wistar* rats after LPS-induced ALI (Fig. 1A). On the other hand, Fig. 1B shows the reduction of relative Bcl-2 mRNA levels in animals subjected to the same conditions. Increased apoptosis rate could also be related to polymorphonuclear cells' presence following LPS administration. This type of cell has an additional mechanism for free radical production and could be more sensitive to photobiomodulation by exposure to a low power infrared laser, inducing the apoptosis process.[49] Our findings agree with another study which describes the selective action of photobiomodulation in different cell types in another inflammation model.[12]

Photobiomodulation results from changes in biochemical reactions and, consequently, in cellular functions following photon absorption by cytochrome c oxidase, which increases ATP synthesis and reactive oxygen species levels[50] as well as positively regulates proliferation and cell death genes.[51] The ALI group presented a significant difference in relative caspase 3 and BCL-2 mRNA levels when compared to the control group. Data normalization for the groups subjected to photobiomodulation was performed with the control group, as well as data normalization for the LPS-induced ALI groups, subjected to photobiomodulation, was performed with the ALI group.

Our findings do not demonstrate changes in relative caspase 3 and Bcl-2 mRNA levels after photobiomodulation by low power infrared laser exposure in control animals (Fig. 2A and 3A). However, in LPS-induced ALI animals, there occur a reduction of caspase 3 mRNA levels and an increase of Bcl-2 mRNA levels by photobiomodulation (Fig. 2B and 3B). It is possible that caspase 3 mRNA levels have already decreased in polymorphonuclear cells in the apoptosis process. In fact, the DNA fragmentation rate from the inflammation area is increased in these animals (Fig. 6). Thus, increasing Bcl-2 mRNA levels could be detected and this could be from the other cell type. Some authors have reported the inflammatory process reduction[52] and Bcl-2 mRNA level increase by photobiomodulation,[12] suggesting that apoptosis is part of the photobiomodulation effects. Other authors have reported that TNF-α/cycloheximide induced apoptosis reduction in endothelial cells exposed to a low power red laser.[53] Following that, photobiomodulation activates NF-κB to induce protection against oxidative stress and apoptosis mediated by caspase-3, which occurs following noise-induced hearing loss induced by photobiomodulation in the ears.[54]

From laser beam absorption by photoacceptors in mitochondria, with subsequent modulation of the redox potential, transcription factors, such as NF-kB, could be induced and act on target genes of the Bcl-2 family of anti-apoptotic members for example. In addition, DNA, RNA and cell cycle regulatory protein acceleration would culminate in cell proliferation promotion and production of oxygen and nitrogen reactive species, which could participate as second messengers in cell signaling pathways[55] or react with DNA, causing damage at the sublethal level.[56,57]

DNA damage, detected by TUNEL assay,[58,59] was correlated with oxidative stress.[60] Human fibroblasts exposed to hydrogen peroxide show condensation of chromatin, changes in mitochondrial membrane potential and increased DNA fragmentation detected by TUNEL.[61] Our results show DNA fragmentation increases in alveolar cells from lung tissue affected by LPS-induced ALI. However, photobiomodulation reduces DNA fragmentation (Fig. 5), mainly at a higher fluence (20 J cm^{-2}). Also, our results suggest that photobiomodulation accelerates polymorphonuclear cell death and protects alveolar cells. Studies have shown the importance of polymorphonuclear cell death by apoptosis in inflammatory diseases, since it marks the beginning of the resolving phase of inflammation,[62–64] which could indicate the action of the photobiomodulation mechanism by low power infrared lasers on acute lung injury.

Conclusion

Our research shows that photobiomodulation by exposure to a low power infrared laser can alter relative mRNA levels in genes involved in the apoptotic process and DNA fragmentation in inflammatory and alveolar cells following acute lung injury induced by lipopolysaccharide. Also, inflammatory cell apoptosis is part of the photobiomodulation effects induced by exposure to a low power infrared laser.

Ethical statement

All experiments were conducted in accordance with the Ethics Committee in Animal Experiments of Universidade Federal de Juiz de Fora, Minas Gerais, Brazil (protocol number 012/2016); the study was registered at Universidade Federal de Juíz de Fora and approved by Pro-Reitoria De Pesquisa/UFJF – Ethical Committee for Animal Handling (CEUA).

Conflicts of interest

The authors declare that there is no conflict of interest regarding the publication of this paper.

Acknowledgements

This work was supported by Conselho Nacional de Desenvolvimento Científico e Tecnológico (CNPq), Fundação Carlos Chagas de Amparo à Pesquisa do Estado do Rio de Janeiro (FAPERJ), Fundação de Amparo à Pesquisa do Estado de Minas Gerais (FAPEMIG).

References

1 D. G. Ashbaugh, D. B. Bigelow, T. L. Petty and B. E. Levine, Acute respiratory distress in adults, *Lancet*, 1967, **2**, 319–323.
2 ARDS Definition Task Force, V. M. Ranieri, G. D. Rubenfeld, B. T. Thompson, N. D. Ferguson, E. Caldwell, E. Fan, L. Camporota and A. S. Slutsky, Acute respiratory distress syndrome: the Berlin Definition, *J. Am. Med. Assoc.*, 2012, **307**, 2526–2533.
3 S. E. Jolley, C. L. Hough, G. Clermont, D. Hayden, S. Hou, D. Schoenfeld, N. L. Smith, B. T. Thompson, G. R. Bernard and D. C. Angus, ARDS Network Investigators, Relationship between race and the effect of fluids on long-term mortality after acute respiratory distress syndrome. Secondary analysis of the national heart, lung, and blood institute fluid and catheter treatment trial, *Ann. Am. Thorac. Soc.*, 2017, **14**, 1443–1449.
4 S. Han and R. Mallampalli, The acute respiratory distress syndrome: From mechanism to translation, *J. Immunol.*, 2015, **194**, 855–860.
5 E. Crimi and A. S. Slutsky, Inflammation and the acute respiratory distress syndrome, *Best Pract. Res., Clin. Anaesthesiol.*, 2004, **18**, 477–492.
6 B. Geering and H. U. Simon, Peculiarities of cell death mechanisms in neutrophils, *Cell Death Differ.*, 2011, **18**, 1457–1469.
7 B. Dibbert, M. Weber, W. H. Nikolaizik, P. Vogt, M. H. Schoni, K. Blaser and H. U. Simon, Cytokine-mediated Bax deficiency and consequent delayed neutrophil apoptosis: a general mechanism to accumulate effector cells in inflammation, *Proc. Natl. Acad. Sci. U. S. A.*, 1999, **96**, 13330–13335.
8 M. E. Peter, Programmed cell death: apoptosis meets necrosis, *Nature*, 2011, **471**, 310–312.
9 S. Elmore, Apoptosis: a review of programmed cell death, *Toxicol. Pathol.*, 2007, **35**, 495–516.
10 J. C. Martinou and R. J. Youle, Mitochondria in apoptosis: Bcl-2 family members and mitochondrial dynamics, *Dev. Cell*, 2011, **21**, 92–101.
11 A. Shamas-Din, J. Kale, B. Leber and D. W. Andrews, Mechanisms of Action of Bcl-2 Family Proteins, *Cold Spring Harbor Perspect. Biol.*, 2013, **5**, a008714.
12 L. M. J. Dos Anjos, A. S. da Fonseca, J. Gameiro and F. de Paoli, Apoptosis induced by low power laser in polymorphonuclear cells of acute joint inflammation: comparative analysis of two energy densities, *Lasers Med. Sci.*, 2017, **32**, 975–983.
13 M. H. Niemz, *Laser-tissue interactions: Fundamentals and applications*, Springer-Verlag, New York, 2007.
14 T. I. Karu, Low-power laser therapy, in *Biomedical photonics handbook*, ed. T. Vo Dinh, CRC Press, Boca Raton, 2003.
15 A. Bartos, Y. Grondin, M. E. Bortoni, E. Ghelfi, R. Sepulveda, J. Carroll and R. A. Rogers, Pre-conditioning with near infrared photobiomodulation reduces inflammatory cytokines and markers of oxidative stress in cochlear hair cells, *J. Biophotonics*, 2016, **9**, 1125–1135.
16 C. Y. Fukuoka, A. Simões, T. Uchiyama, V. E. Arana-Chavez, Y. Abiko, N. Kuboyama and U. K. Bhawal, The Effects of Low-Power Laser Irradiation on Inflammation and Apoptosis in Submandibular Glands of Diabetes-Induced Rats, *PLoS One*, 2017, **12**, e0169443.
17 M. Gulsoy, G. H. Ozer, O. Bozkulak, H. O. Tabakoglu, E. Aktas, G. Deniz and C. Ertan, The biological effects of 632.8 nm low energy HeNe laser on peripheral blood mononuclear cells in vitro, *J. Photochem. Photobiol., B*, 2006, **82**, 199–202.
18 N. A. Pereira, C. P. Eduardo, E. Matson and M. M. Marques, Effect of low-power laser irradiation on cell growth and procollagen synthesis of cultured fibroblasts, *Lasers Surg. Med.*, 2002, **31**, 263–267.
19 A. Dube, H. Bansal and P. K. Gupta, Modulation of macrophage structure and function by low level He-Ne laser irradiation, *Photochem. Photobiol. Sci.*, 2003, **2**, 851–855.
20 J. V. Kruchenok, S. B. Bushuk, G. I. Kurilo, N. A. Nemkovich and A. N. Rubinov, Orientation of red blood cells and roleaux disaggregation in interference laser fields, *J. Biol. Phys.*, 2005, **31**, 73–85.
21 A. K. Schroder, M. von der Ohe, U. Kolling, J. Alstaedt, P. Uciechowski, D. Fleischer, K. Dalhoff, X. Ju, M. Zenke, N. Heussen and L. Rink, Polymorphonuclear leucocytes selectively produce anti-inflammatory interleukin-1 receptor antagonist and chemokines, but fail to produce pro-inflammatory mediators, *Immunology*, 2006, **119**, 317–327.
22 S. M. Safavi, B. Kazemi, M. Esmaeili, A. Fallah, A. Modarresi and M. Mir, Effects of low level He-Ne laser irradiation on the gene expression of IL-1β, TNF-α, IFN-γ, TGF-β, bFGF and PDGF in rat's gingiva, *Lasers Med. Sci.*, 2008, **23**, 331–335.
23 N. A. Zhevago and K. A. Samoilova, Pro- and anti-inflammatory cytokine content in human peripheral blood alter its transcutaneous (in vivo) and direct (in vitro) irradiation with polychromatic visible and infrared light, *Photomed. Laser Surg.*, 2006, **24**, 129–139.
24 D. L. Brown, Practical Stereology Applications for the Pathologist, *Vet. Pathol.*, 2017, **54**, 358–368.
25 K. J. Livak and T. D. Schmittgen, Analysis of relative gene expression data using real-time quantitative PCR and the 2(-Delta Delta C(T)), Method, *Methods*, 2001, **25**, 402–408.

26 W. Lim, S. Lee, I. Kim, M. Chung, M. Kim, H. Lim, J. Park, O. Kim and H. Choi, The anti-inflammatory mechanism of 635 nm lightemitting-diode irradiation compared with existing COX inhibitors, *Lasers Surg. Med.*, 2007, **39**, 614–621.

27 P. R. Arany, Craniofacial wound healing with photobiomodulation therapy: new insights and current challenges, *J. Dent. Res.*, 2016, **95**, 977–984.

28 P. Rola, A. Doroszko and A. Derkacz, The Use of Low-Level Energy Laser Radiation in Basic and Clinical Research, *Adv. Clin. Exp. Med.*, 2014, **23**, 835–842.

29 F. B. Fiorio, S. A. dos Santos, C. S. de Melo Rambo, C. G. Dalbosco, A. J. Serra, B. L. de Melo, E. C. P. Leal-Junior and P. T. C. de Carvalho, Photobiomodulation therapy action in wound repair skin induced in aged rats old: time course of biomarkers inflammatory and repair, *Lasers Med. Sci.*, 2017, **8**, 1769–1782.

30 A. R. de Oliveira, A. A. Vanin, S. S. Tomazoni, E. F. Miranda, G. M. Albuquerque-Pontes, T. de Marchi, V. dos Santos Grandinetti, P. R. V. de Paiva, T. B. G. Imperatori, P. T. C. de Carvalho, J. M. Bjordal and E. C. P. Leal-Junior, Pre-Exercise Infrared Photobiomodulation Therapy (810 nm) in Skeletal Muscle Performance and Postexercise Recovery in Humans: What Is the Optimal Power Output?, *Photomed. Laser Surg.*, 2017, **11**, 595–603.

31 Y. Shen, C. Xie, Y. Gu, X. Li and J. Tong, Illumination from light-emitting diodes (LEDs) disrupts pathological cytokines expression and activates relevant signal pathways in primary human retinal pigment epithelial cells, *Exp. Eye Res.*, 2016, **145**, 456–467.

32 Y. Oshima, R. D. Coutts, N. M. Badlani, R. M. Healey, T. Kubo and D. Amiel, Effect of light-emitting diode (LED) therapy on the development of osteoarthritis (OA) in a rabbit model, *Biomed. Pharmacother.*, 2011, **3**, 224–229.

33 Y. Oshima, R. D. Coutts, N. M. Badlani, R. M. Healey, T. Kubo and D. Amiel, Effect of light-emitting diode (LED) therapy on the development of osteoarthritis (OA) in a rabbit model, *Biomed. Pharmacother.*, 2011, **3**, 224–229.

34 K. R. Byrnes, R. W. Waynant, I. K. Ilev, X. Wu, L. Barna, K. Smith, R. Heckert, H. Gerst and J. J. Anders, Light promotes regeneration and functional recovery and alters the immune response after spinal cord injury, *Lasers Surg. Med.*, 2005, **3**, 171–185.

35 T. A. Henderson and L. D. Morries, Near-infrared photonic energy penetration: can infrared phototherapy effectively reach the human brain?, *Neuropsychiatr. Dis. Treat.*, 2015, **11**, 2191–2208.

36 D. E. Hudson, D. O. Hudson, J. M. Wininger and B. D. Richardson, Penetration of laser light at 808 and 980 nm in bovine tissue samples, *Photomed. Laser Surg.*, 2013, **4**, 163–168.

37 F. Bortone, H. A. Santos, R. Albertini, J. B. Pesquero, M. S. Costa and J. J. Silva, Low level laser therapy modulates kinin receptors mRNA expression in the subplantar muscle of rat paw subjected to carrageenan-induced inflammation, *Int. Immunopharmacol.*, 2008, **8**, 206–210.

38 O. Lesur, A. Kokis, C. Hermans, T. Fulop, A. Bernard and D. Lane, Interleukin-2 involvement in early acute respiratory distress syndrome: relationship with polymorphonuclear neutrophil apoptosis and patient survival, *Crit. Care Med.*, 2000, **28**, 3814–3822.

39 V. Galani, E. Tatsaki, M. Bai, P. Kitsoulis, M. Lekka, G. Nako and P. Kanavaros, The role of apoptosis in the pathophysiology of Acute Respiratory Distress Syndrome (ARDS): an up-to-date cell-specific review, *Pathol., Res. Pract.*, 2010, **206**, 145–150.

40 R. H. Bardales, S. S. Xie, R. F. Schaefer and S. M. Hsu, Apoptosis is a major pathway responsible for the resolution of type II pneumocytes in acute lung injury, *Am. J. Pathol.*, 1996, **149**, 845–852.

41 T. R. Martin, N. Hagimoto, M. Nakamura and G. Matute-Bello, Apoptosis and Epithelial Injury in the Lungs, *Proc. Am. Thorac. Soc.*, 2005, **2**, 214–220.

42 K. H. Kim, M. J. Kwun, C. W. Han, K. T. Kan, J. Y. Choi and M. Joon, Suppression of lung inflammation in an LPS-induced acute lung injury model by the fruit hull of Gleditsia sinensis, *BMC Complementary Altern. Med.*, 2014, **14**, 402–409.

43 C. M. Gross, M. Kellner, T. Wang, Q. Lu, X. Sun, E. A. Zemskov, S. Noonepalle, A. Kangath, S. Kumar, M. Gonzalez-Garay, A. A. Desai, S. Aggarwal, B. Gorshkov, C. Klinger, A. D. Verin, J. D. Catravas, J. R. Jacobson, J. X. Yuan, R. Rafikov, J. G. N. Garcia and S. M. Black, LPS Induced Acute Lung Injury Involves the NF-κB-mediated Downregulation of SOX18, *Am. J. Respir. Cell Mol. Biol.*, 2017, **5**, 614–624.

44 B. Zhu, G. H. Luo, Y. H. Feng, M. M. Yu, J. Zhang, J. Wei, C. Yang, N. Xu and X. Y. Zhang, Apolipoprotein M Protects Against Lipopolysaccharide-Induced Acute Lung Injury via Sphingosine-1-Phosphate Signaling, *Inflammation*, 2018, **2**, 643–653.

45 N. Liu, X. Ma, X. Luo, Y. Zhang, Y. He, Z. Dai, Y. Yang, G. Wu and Z. Wu, l-Glutamine Attenuates Apoptosis in Porcine Enterocytes by Regulating Glutathione-Related Redox Homeostasis, *J. Nutr.*, 2018, **4**, 526–534.

46 R. D. Barber, D. W. Harmer, R. A. Coleman and B. J. Clark, GAPDH as a housekeeping gene: analysis of GAPDH mRNA expression in a panel of 72 human tissues, *Physiol. Genomics*, 2005, **21**, 398–395.

47 Z. Darzynkiewicz, D. Galkowski and H. Zhao, Analysis of apoptosis by cytometry using TUNEL assay, *Methods*, 2008, **3**, 250–254.

48 D. T. Loo, In situ detection of apoptosis by the TUNEL assay: an overview of techniques, *Methods Mol. Biol.*, 2011, **682**, 3–13.

49 Y. Y. Huang, A. C. H. Chen, J. D. Carroll and M. R. Hamblin, Biphasic dose response in low level light therapy, *Dose-Response*, 2009, **7**, 358–383.

50 T. I. Karu, Multiple roles of cytochrome c oxidase in mammalian cells under action of red and IR-A radiation, *IUBMB Life*, 2010, **62**, 607–610.

51 T. I. Karu, Mitochondrial signaling in mammalian cells activated by red and near-IR radiation, *Photochem. Photobiol.*, 2008, **84**, 1091–1099.
52 P. C. Silveira, K. B. Ferreira, F. R. da Rocha, B. L. Pieri, G. S. Pedroso, C. T. De Souza, R. T. Nesi and R. A. Pinho, Effect of Low-power laser (LPL) and light-emitting diode (LED) on inflammatory response in burn wound healing, *Inflammation*, 2016, **39**, 1395–1404.
53 Y. H. Chu, S. Y. Chen, Y. L. Hsieh, Y. H. Teng and Y. J. Cheng, Low-level laser therapy prevents endothelial cells from TNF-α/cycloheximide-induced apoptosis, *Lasers Med. Sci.*, 2018, **33**, 279–286.
54 A. Tamura, T. Matsunobu, R. Tamura, S. Kawauchi, S. Sato and A. Shiotani, Photobiomodulation rescues the cochlea from noise-induced hearing loss via upregulating nuclear factor κB expression in rats, *Brain Res.*, 2016, **1646**, 467–474.
55 Y. Shingyochi, S. Kanazawa, S. Tajima, R. Tanaka, H. Mizuno and M. Tobita, A Low-Level Carbon Dioxide Laser Promotes Fibroblast Proliferation and Migration through Activation of Akt, ERK, and JNK, *PLoS One*, 2017, **12**, e0168937.
56 A. S. Fonseca, T. O. Moreira, D. L. Paixão, F. M. Farias, O. R. Guimarães, S. Paoli, M. Geller and F. Paoli, Effect of laser therapy on DNA damage, *Lasers Surg. Med.*, 2010, **42**, 481–488.
57 E. Schulz, P. Wenzel, T. Münzel and A. Daiber, Mitochondrial redox signaling: interaction of mitochondrial reactive oxygen species with other sources of oxidative stress, *Antioxid. Redox Signaling*, 2014, **20**, 308–324.
58 V. M. Heatwole, TUNEL assay for apoptotic cells, *Methods Mol Biol.*, 1999, **115**, 141–148.
59 K. Kyrylkova, S. Kyryachenko, M. Leid and C. Kioussi, Detection of apoptosis by TUNEL assay, *Methods Mol. Biol.*, 2012, **887**, 41–47.
60 S. Lopes, A. Jurisicova, J. G. Sun and R. F. Casper, Reactive oxygen species: potential cause for DNA fragmentation in human spermatozoa, *Hum. Reprod.*, 1998, **13**, 896–900.
61 P. Formichi, E. Radi, C. Battisti, E. Tarquini, A. Leonini, A. Di Stefano and A. Federico, Human fibroblasts undergo oxidative stress-induced apoptosis without internucleosomal DNA fragmentation, *J. Cell Physiol.*, 2006, **208**, 289–297.
62 F. Aimbire, F. V. Santos, R. Albertini, H. C. Castro-Faria-Neto, J. Mittmann and C. Pacheco-Soares, Low-level laser therapy decreases levels of lung neutrophils anti-apoptotic factors by a NF-kappaB dependent mechanism, *Int. Immunopharmacol.*, 2008, **8**, 603–605.
63 D. El Kebir and J. G. Filep, Role of neutrophil apoptosis in the resolution of inflammation, *Sci. World J.*, 2010, **10**, 1731–1748.
64 C. Miranda da Silva, M. Peres Leal, R. A. Brochetti, T. Braga, L. B. Vitoretti, N. O. Saraiva Câmara, A. S. Damazo, A. P. Ligeiro-deOliveira, M. C. Chavantes and A. Lino-Dos-Santos-Franco, Low level laser therapy reduces the development of lung inflammation induced by formaldehyde exposure, *PLoS One*, 2015, **10**, e0142816.